Algal Research 71 (2023) 103028

Contents lists available at ScienceDirect

Algal Research

journal homepage: www.elsevier.com/locate/algal

Hydrodynamics of an integrated fish and periphyton recirculating aquaculture system

Adam N. Bell [a], Lior Guttman [b], Kevan L. Main [c], Michael Nystrom [c], Nathan P. Brennan [c], Sarina J. Ergas [a,*]

[a] Department of Civil and Environmental Engineering, University of South Florida, USA
[b] Israel Oceanographic and Limnological Research, The National Center for Mariculture, 8811201 Eilat, Israel
[c] Mote Aquaculture Research Park, Mote Marine Laboratory, Sarasota, FL, USA

ARTICLE INFO

Keywords:
Periphyton
Integrated multi-trophic aquaculture
Biofilter
Nutrient removal
Recirculating aquaculture system

ABSTRACT

Marine aquaculture helps to mitigate a number of environmental problems, such as overfishing, loss of biodiversity, and eutrophication. Periphyton-based biofilters are a promising technology for marine aquaculture water treatment because periphyton repurposes nutrients as fish feed and produces dissolved oxygen (DO). Integration of periphyton biofilters into recirculating aquaculture systems (RAS) also preserves water and prevents pollutant discharges. In this study, we examined the effect of system hydrodynamics on two pilot-scale (2500 L) RAS with integrated periphyton biofilters, which were used to grow *Ariopsis felis* (hardhead catfish). Periphyton was harvested weekly from hanging nets. Conservative tracer tests conducted at varying fluid velocities indicated the presence of dead zones along tank edges. Growth of periphyton biomass was found to be primarily dependent on the nutrient mass loading rate. Improved mass transport and uptake of aqueous nutrients by periphyton occurred at higher fluid velocities. DO production by periphyton photosynthesis also increased with increasing fluid velocities. Mass balances on C, N, and DO were carried out to elucidate the nutrient transformation pathways and quantities. DO analysis revealed that periphyton provided 1.31 ± 0.20 mg DO/(L*m^2*day) during daytime hours. This was nearly enough to support microbial and fish respiration without the use of a blower. Periphyton and filamentous algae, *Oscillatoriaceae*, removed 32 ± 4 % of the input nitrogen and 61 ± 3 % of input carbon from the feed that was not taken up by the cultured fish. The overall water quality goals for the catfish were either met or exceeded through application of periphyton biofilters in the RAS.

1. Introduction

Aquaculture production of marine plants and animals can provide sustainable options for an increasing global population with high demands for seafood. Monoculture of fish is limited by factors related to the food-water-energy nexus, such as water availability and discharges of organic matter, solids, and nutrients to the environment. Recirculating aquaculture systems (RAS) provide a way to grow fish or shellfish at a high density while conserving water and land, reducing pollution discharges, and controlling water quality for fish health. Disadvantages of RAS include high energy requirements [1], burden-shifting from local to global environmental impacts [2], and costs of water treatment [3].

The concept of integrated multi-trophic aquaculture (IMTA) involves farming several species from different trophic levels [4]. In many cases, the waste from one species is the substrate for another, as in farming an extractive algal species in fishpond effluent using excreted aqueous nutrients. Such extractive species can increase the commercial value of marine seafood production and can provide carbon trading credits [5]. Besides mitigating wasted nutrients, the produced periphyton can be used as a nutritious edible feed when provided fresh in the diet of fish or shrimps [6–8].

Periphyton is a complex aquatic community of macro- and microalgae, bacteria, and fauna that grows on a submerged substratum and is influenced by light and nutrients [9]. The substratum can be organic, such as bamboo, or inorganic, such as glass [10]. An integrated finfish culture with periphyton is traditionally known as *kathas* in Bangledesh, *acadjas* in Benin, and *aji gnui assonii* in India [11]. Recent studies confirmed periphyton's efficiency in the biofiltration of fishpond effluent in marine IMTAs; the periphyton-based biofilter improved water quality parameters related to fish health, such as total ammonia

* Corresponding author at: Department of Civil and Environmental Engineering, University of South Florida, 4202 E Fowler Avenue, Tampa, FL 33620, USA.
E-mail address: sergas@usf.edu (S.J. Ergas).

https://doi.org/10.1016/j.algal.2023.103028
Received 9 November 2022; Received in revised form 16 January 2023; Accepted 15 February 2023
Available online 20 February 2023

nitrogen (TAN), nitrate (NO_3^-), nitrite (NO_2^-), dissolved oxygen (DO), pH, and carbon dioxide (CO_2) [12–14]. Algae have evolved diverse carbon concentrating mechanisms to sequester both HCO_3^- and CO_2 [15]. It was found that periphyton biofilters rapidly remove TAN [16]. When TAN concentrations decreased below 0.3 mg/L, NO_3^- was removed at a rate of 1.4 g NO_3^--N/(m^2*d). The simultaneous uptake of these N forms is likely due to the co-occurrence of algae and bacteria in the periphyton [17,18]. The rapid uptake of NO_3^- makes the periphyton biofilter particularly promising for application in RAS, where NO_3^- accumulation is common even when using a denitrifying biofilter [19,20]. Periphyton harvested from an IMTA was shown to successfully replace 50 % of the fishmeal in the diet of the carnivore gilthead sea bream (*Sparus aurata*) [21], reducing the climate impacts of aquafeeds by incorporating algae ingredients [22]. Microalgae, such as those in the periphyton [23], are also excellent candidates for replacing fish oil in aquafeeds, due to their synthesis of essential Ω-3 fatty acids [24]. Alternatively, harvesting algae in periphyton can have varied applications including biofuel, biochar, fertilizer, and cosmetics [25].

Algal turf scrubbers (ATS) are a related type of attached growth algae treatment system that has been used to treat municipal [26], agricultural [27], and industrial [28] wastewater. ATS grow algae in shallow substratum lined floways that are directly exposed to sunlight and subject to oscillating hydraulic loads [29,30]. Algal biomass provide both wastewater treatment and DO and are harvested from ATS every one to two weeks [31]. Two commercial RAS treated by ATS are described in the literature: one nearly closed system producing 600,000–800,000 lbs./year of freshwater tilapia and a second closed RAS producing 900,000 lbs./year of tilapia and hybrid striped bass [32]. Periphyton biofilters have been utilized in marine [12] and brackish (this study) RAS compared with ATS, which have only been reported for use in freshwater aquaculture applications [32].

Understanding the relationship between the hydrodynamic flow of nutrients and biofiltration performance is crucial for developing periphyton biofilters for RAS. In a closed system, hydraulic residence time (HRT) can significantly influence periphyton according to three mechanisms: the diffusive flux of dissolved gases (CO_2, DO), dispersion of aqueous nutrients (N, P, C), and sloughing of biomass. Hydrodynamic dispersion occurs because of the inertia due to water flow past a rough surface, the change in water volume relative to the surface area of flow through a substratum, and the available path that a fluid can potentially move through a substratum [33]. Under low-velocity conditions, the transfer of nutrients from the bulk fluid to periphyton occurs through the liquid-periphyton boundary layer, mostly by Taylor dispersion [34]. Concentrations of nutrients, such as CO_2, have been shown to decrease exponentially through the boundary layer, from about 2 mm into the bulk fluid to the periphyton surface [35]. Once nutrients are transferred to periphyton, growth and nutrient uptake occur in several phases. First, growth increases rapidly by Monod kinetics and second, growth increases linearly up to a saturation point as nutrient transfer is limited by dispersion [36]. The density of periphyton further inhibits dispersion [37].

Periphyton harvesting and function are also affected by hydrodynamics. A regular weekly harvesting regime improved the biomass growth rate and nitrogen removal for a filamentous periphyton community treating anaerobically digested food waste filtrate [38]. The removal rate of total inorganic N by periphyton biosynthesis was proportional to periphyton yield and reached a maximum after six weeks [23]. Therefore, a regular harvest regime is needed to control periphyton's growth, biofiltration, and gain an extractive IMTA product.

The goal of this study was to understand the effect of system hydrodynamics on the performance of RAS-periphyton biofilters. Two new pilot-scale RAS with periphyton biofilters were designed, constructed, and operated with brackish water. The effect of system hydrodynamics on water quality, harvest yields, nutrient balance, and mass transport in the RAS was investigated.

2. Materials and methods

2.1. Design and construction

The study was carried out at Mote Aquaculture Research Park (Sarasota, FL, USA). The design of the brackish RAS with periphyton biofilters was based on the water quality requirements for fish health (Table 1). The pilot-scale (Fig. 1; V_b = 2500 ± 10 L) system was designed based on a review of prior periphyton aquaculture systems [12,23,39]. The biofilter was designed as four completely mixed flow reactors (CMFRs) in series. Recirculation flow rates were designed to be adjustable to change the areal loading rate (mg nutrient/(m^2*h)) on the substratum.

Construction of RAS 1 took place in June of 2021; RAS 2 was constructed in March of 2022. The RAS were built to be as close to identical as possible. Each RAS contained a cylindrical 1150 L tank (diameter = 156 ± 1 cm, depth = 60.0 ± 0.5 cm) equipped with a submersible Little Giant 5MSP (Fort Wayne, IN, USA; 0.12 kW power, 73.5 Lpm, 1 m head) pump placed in the culture tank. The culture tank operational volume (V_c) was 924 L. Effluent flow from the culture tank was routed between parallel loops: a return line to the culture tank, a clarifier, and the periphyton biofilter series (Fig. 1). The flow rate in each loop was adjusted by using ball valves. The periphyton biofilters were constructed from four cuboid shaped tanks in series (height = 54.0 ± 1.0 cm, length = 104.0 ± 0.5, width = 66.5 ± 0.5 cm, working volume 375 L). The total biofilter volume (V_b) was 1500 L. The influent was distributed into each biofilter tank using a 3.8 cm diameter perforated pipe capped on the end (holes of 0.5 cm, 6 cm apart). As shown in Fig. 1, six high-density polyethylene nets were suspended within each biofilter tank (net SA to water SA of 5:1) as the periphyton substratum. The nets were attached to overhanging pipes using plastic zip-ties. Each net had a thickness of 1 mm, with elliptical holes (major = 4.09 mm by minor = 3.47 mm) and a surface area of 0.588 m^2/net for a total biofilter net surface area of 14.1 m^2. Aeration was provided using a Sweetwater S-53 1.9 kW blower (Sebring, FL, USA). Each clarifier (or settling tank) was constructed using a 75.7 L tank with influent and effluent ports at the top and solids tap on the bottom. The clarifier was operated at an overflow rate of 1.8 ± 0.1 m/h. The flow back into the culture tank ranged between 60 and 65 Lpm depending on the biofilter HRT.

2.2. Experimental design

The investigation was carried out in two phases. Phase I (Summer/Fall 2021) was carried out with a single RAS dosed with synthetic wastewater. Synthetic wastewater was added daily and was composed of 35.0 ± 0.1 g of ground Purina Aquamax Sportfish 600 (3 mm), 1.20 g of NH_3-N, and 8.73 g of $NaHCO_3$ based on previously tested ratios [46]. In Phase I, the following HRTs were tested for each biofilter tank: 1.0 ± 0.2 h, 2.0 ± 0.2 h, 4.0 ± 0.2 h, 6.0 ± 0.2 h, and 8.0 ± 0.2 h. During Phase II, RAS1 and RAS2 were stocked with fish (Summer/Fall 2022) and operated at a HRT of 1.0 ± 0.2 h per biofilter tank. Details of fish stocking, feeding, and handling (according to IACUC guidelines) during Phase II are described in Section (§) 2.6. For both phases, the experiment was set up so that the only parameter contributing to the areal mass loading rate

Table 1
Target water quality values for brackish RAS.

Parameter	Concentration	Reference
DO	>5 mg/L	[40]
TAN	<0.8 mg TAN as N/L	[3]
NH_3	<0.16 mg NH_3 as N/L	[41]
NO_2^-	<5.0 mg NO_2^- as N/L	[42]
NO_3^-	<500 mg NO_3^- as N/L	[43]
Free CO_2	<20. mg/L	[44]
pH	6.5 to 9.0	[45]
Alkalinity	50 to 200 mg $CaCO_3$/L	[45]

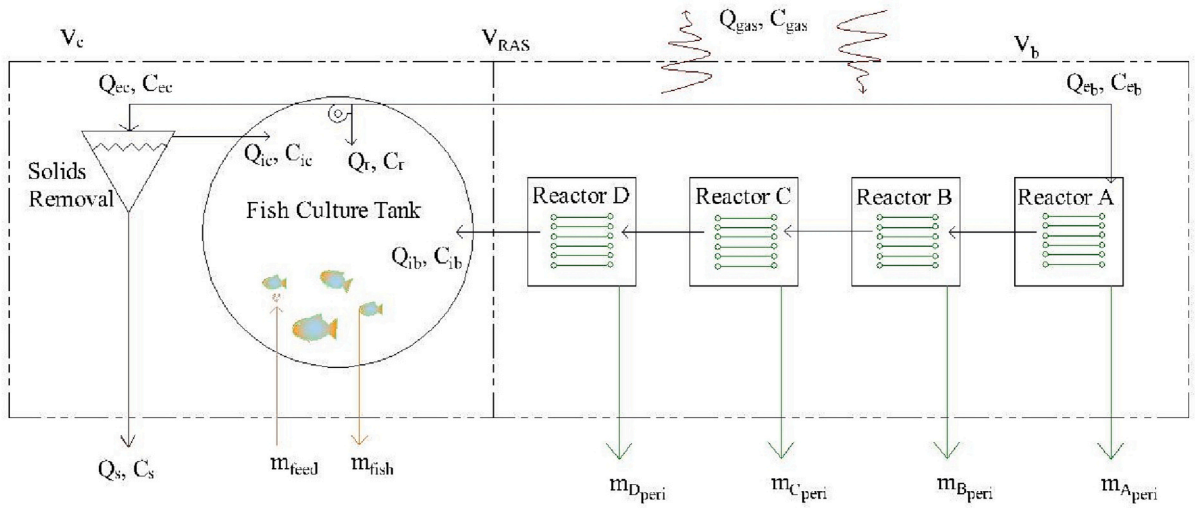

Fig. 1. Schematic diagram of the constructed RAS with periphyton biofilters. Water flows from the culture tank to Reactor A (1 meter head pressure), then gravity-flows sequentially through the remaining biofilters (Reactor B, C, D) to the culture tank. Variables used in mass balance: Q = flow, C = concentration, m = mass transfer; and subscripts: ec = effluent to clarifier, s = solids, ic = influent from clarifier, r = return from pump, eb = effluent to biofilter, ib. = influent from biofilter, m_{Aperi} = periphyton harvested from tank A, m_{Bperi} = periphyton harvested from tank B, m_{Cperi} = periphyton harvested from tank C, m_{Dperi} = periphyton harvested from tank D.

was HRT.

2.3. System startup and fish stocking

System startup was necessary prior to introducing fish so that the biofilter periphyton community could acclimate and approach steady-state. The RAS was filled with freshwater from a deep well and mixed with Instant Ocean (Blacksburg, VA, USA) to achieve a brackish salinity of 15.0 ppt. The effect of evaporation was offset by filling with freshwater weekly. After RAS1 was filled, a 100 mL inoculum from a *Sciaenops ocellatus* (red drum) tank was introduced to provide a microbial inoculum. RAS2 was started using periphyton nets from RAS1. Both RAS were equilibrated over a 1-month period using synthetic wastewater.

Prior to Phase II (June 24–30, 2022), wild hardhead catfish were collected (n = 26, 267 ± 116 g), weighed and measured. The catfish were stocked at a rate 3.8 ± 0.1 kg/m^3 and fed Skretting Europa 18 (6-mm; 50 % protein, 18 % lipids; Stavanger, Norway). The catfish were initially fed a maintenance diet of 1 % body weight per day, which was raised to 2 % at the official start of Phase II on August 22, 2022. Fish survival was recorded throughout the experiment. At the end of Phase II on September 20, 2022, the fish were reweighed and measured to calculate food conversion ratios (FCR) and specific growth rates (SGR).

2.4. Mass transport

Measurement of the influent flow rate used several redundant procedures: Minol Minomess 130 (Addison, TX, USA) flow meter electronically connected to a HOBO datalogger and by timing the fill rate of a 2.0 L graduated cylinder. Velocity measurements were obtained with an OTT MF FP111 flow probe (Kempton, Germany). To measure the mass flux through the biofilter and deviations from the ideal HRT, a conservative tracer study was carried out on each tank at the HRT that corresponded to 1 h in tank A (6.25 Lpm). The tracer study utilized a premixed concentrated salt solution following the method of Calkins and Dunne [47]. The conservative tracer was a concentrated salt solution that was poured into a port on the tank A inlet distributer. The response was measured in 30-second intervals using a YSI ProDSS (Yellow Springs, OH, USA) conductivity meter. The time and concentration were normalized as outlined in Crittenden et al. [48]. To find the baseline of integration, a tracer study was first run at the point of maximum recirculation. The experimental tracer HRTs were compared to the theoretical HRT and to the tanks in series (TIS) model given by Crittenden et al. [48]. The adjusted root mean squared velocity gradient $\overline{G}$ values were calculated using volume, viscosity, and energy dissipation to measure mixing in the reactor [49] and compared with $\overline{G}$ values found in the literature [50]. To observe short-circuits or no-flow (or "dead") zones in the reactor, a qualitative tracer study was also conducted using a Bluewater Chemgroup green tracer dye (Fort Wayne, IN, USA). The gradation of feed solids into the system was quantified by measuring with 600 μm, 300 μm, 100 μm, 35 μm, and 0.45 μm sieves to divide the input into particulate species of varying sizes.

2.5. Periphyton biomass

A modular harvest routine was used to ensure that at any time at least one biofilter tank contained fresh periphyton in exponential growth phase. The routine assumed that periphyton peak biomass occurs sometime between 4 and 6 weeks [23,39]. Harvesting was carried out weekly, sequentially following the tank number (e.g., during week one, the first tank was harvested, during week four, the fourth tank was harvested). Harvesting was carried out by pressure washing the nets through a sieve into a settling container. The fluid in the container was allowed to settle for 1 h, then decanted, and the solids removed with a 100-micron net. During harvest, samples were collected for examination on an Olympus BX53 (Tokyo, Japan) microscope. The solids in the reactor were partitioned between the benthic fraction and periphyton. Additionally, filamentous algae were found to overgrow regularly on top the nets—which would block light— therefore the filamentous algae was removed as needed.

The sampling procedures for measurements of biomass dry weight (DW) and ash-free dry weight (AFDW) were based on ASTM STP 690 [9] and APHA 10300 B [51], with modifications due to the periphyton substratum [39]. The carbon content was approximated as the volatile solids (VS), found by taking the difference between DW and AFDW. The HDPE net material was cut into sample strips (SA = 0.018 ± 0.001 m^2) and suspended in biofilter tank A. The sample strips were harvested in duplicate at 11, 14, 18, 21 days in Phase I. Sampling in Phase II was changed to day 7, 14, 21, 28 days to better quantify the growth curve. The strips were placed on a Fischer Scientific No. 7 sieve (Pittsburgh, PA, USA), then pressure washed from the strip into a container. The sample

was transferred to a 1.0 L graduated cylinder and allowed to settle for 1 h. The cylinder was decanted into two fractions, the settled solids, and the bulk fluid. The bulk fluid was passed through a 35-micron mesh. Both caught and settled solids were transferred to pans, and dried at 105 °C for 24 h in a VWR gravity convection oven (Radnor, PA, USA). The resulting biomass yields were then either tabulated or plotted.

2.6. Water quality analysis

Measurements of pH, salinity, temperature, and DO were taken at least 3 times per week. The pH and salinity of the water were measured using a YSI Inc. handheld ProDSS (Yellow Springs, OH, USA) conductivity meter. The DO and temperature were also data-logged using a HACH sc1000 controller with an optical dissolved oxygen LDO model II sensor in RAS 1. The photosynthetically active radiation (PAR) was datalogged on an Onset HOBO microstation H21 USB (Bourne, MA, USA) or by Apogee MQ-200 (North Logan, UT, USA). The light measurement with the handheld Apogee was taken by placing the sensor gently in the center of the tank and lowering to the target depth. The alkalinity (APHA 2320) and BOD_5 (APHA 5210-B) were normally measured once per week. In Phase II, CO_2 samples were taken at least once per week. The samples were measured for initial free gas CO_2 using an Oxyguard handheld CO_2 analyzer (Farum, Denmark). Carbonate carbon was found by titrating the solution to pH 4.5 using 0.1 N HCl then measuring the free CO_2.

Water samples were collected twice per week at 13:00 for analysis of NO_3^-, NO_2^-, and TAN in Phase I, and once per week for Phase II. Samples were filtered using 0.45 μm pore size filter. TAN was measured using a TL-2800 Timberline (Keenesburg, CO) ammonia analyzer. The sum of NO_3^- and NO_2^- was measured with the zinc reduction method [52]. NO_2^- was measured on a Gensys 10uv Thermo Electron (Millersburg, PA) spectrophotometer by APHA 4500-NO_2^-. The total nitrogen content of feeds and solids were obtained by ASTM D5762 - 18a [53] using a Thermo TN3000 total nitrogen analyzer.

2.7. Data analysis and mass balances

In the R programming environment [54], the distributions and test assumptions for each test were first checked (e.g., Shapiro Wilk for normality, F-test for normality). Paired *t*-tests were used in Phase I when comparing trials, because the HRT trials were run on the same RAS. The parameter set for each HRT was tested by enumerating the HRTs (e.g. TAN in HRT1 against TAN in HRT2). Phase II contained a replicate; thus, the results were not paired. Unpaired t-tests were applied for critical p values < 0.05 unless otherwise specified. Alternatively, single factor ANOVA was used when comparing Phase I to RAS1 and RAS2. The Kruskal-Wallis signed rank test was applied when the normality assumption was not met. Linear regression was applied as needed.

The nutrient mass balances were performed using the methods and measurements in §2.3 to 2.5, with Fig. 1 as a guide. The equations generally followed the form:

$$V\left(\frac{dC}{dt}\right) = m_{feed} - m_{peri} - m_{fish} - m_{benth} \pm QC_{org} \pm QC_{inorg} \pm JA \pm V\sum r \quad (1)$$

The particulate mass terms, m (units of mass/time), include feed, periphyton, fish, and benthic or settled solids. Aqueous nutrients are generally partitioned between the inorganic and organic fractions and are measured by the product of the flow rate (Q) and concentration (C). Two-film theory was used to describe the mass flux of gases (J, units' mass/(time*area)) by the expression $K_LA(C^* - C\ (t))$ multiplied by the reactor volume V to get to units of mass per time [55]. The mass transfer coefficient is $K_L\left(\frac{1}{time^*area}\right)$ while A is the surface area where the gas flux occurs. The term $C\ (t)$ is the concentration of the gas in solution. The difference $(C^* - C\ (t))$ indicates the magnitude of the driving force for gas transfer. The sum of the reactions is given by $\sum r$ (units' mass/(volume*time)). Water quality calculations such as the alkalinity speciation were ascertained using Visual MINTEQ [56]. The difference between the amount of nutrient added into the RAS as feed and the amount of nutrient taken up by the culture species is referred to as the extractive portion of N or C. The data for the mass balances was collected in Phase II for a HRT of 1 h unless otherwise specified.

Nitrogen accumulation is summarized by Eq. (2):

$$\frac{VdC(N)}{dt} = m_{N,feed} - m_{N,fish} - m_{N,peri} - m_{benth} \pm QC_{N,TIN} \pm QC_{N,DON} - Vr_{denit} \pm Vr_{DON} \pm Vr_{ammon} \pm Vr_{uptake,TIN} \pm Vr_{uptake,DON} \quad (2)$$

The total change in nitrogen mass is described by the product of the volume and the concentration of nitrogen (C(N)) in the RAS. The aqueous fractions of total inorganic nitrogen (TIN) and dissolved organic nitrogen (DON) were used to partition inorganic and organic fractions. The dissolution of feed is described by r_{DON}. The ammonification of organic feed, r_{ammon}, is the reaction that controls the conversion of DON to TIN. The denitrification rate r_{denit} was solved for empirically by measuring the total nitrogen of each term and assuming steady state. The reaction pathway out of the reactor (r_{denit}) includes the sum of denitritation ($NO_2^- \rightarrow N_2$), denitrification ($NO_3^- \rightarrow N_2$), and anammox ($NH_4^+ + NO_2^- \rightarrow N_2$). Denitrification is the conventional method of removing NO_3^--nitrogen in RAS, although denitritation is also a thermodynamically and ecologically favorable reaction path for phototrophic/heterotrophic removal of NO_2^- from wastewater [57]. The alternative pathway for removal of TIN is through biosynthesis into periphyton mass, which is described by $r_{uptake,\ TIN}$. Alternatively, algae can grow on organic nitrogen sources, particularly on simple DON species such as urea when the TIN concentration is low [58].

Dissolved oxygen accumulation is summarized by Eq. (3):

$$\frac{VdC(DO)}{dt} = \pm VK_{L,mech}A\left(C^*_{DO} - C\ (t)\right) \pm VK_{L,inlet}A\left(C^*_{DO} - C\ (t)\right) + Vr_{DO,photo} - Vr_{DO,resp} \quad (3)$$

The total change in DO mass is described by the product of the volume and the DO concentration per increment of time. Eq. (3) is non-steady state due to the effect of diel light cycles on photosynthesis. Accumulation was measured using the HACH datalogger with LDO sensor placed in culture tank. The major variables included were the influx/efflux of oxygen in and out of the reactor surface area due to the mechanical blower ($K_{L,\ mech}A$) and inlet distributer ($K_{L,\ inlet}A$), the oxygen uptake due to microbial and fish demand ($r_{DO,\ resp}$), and the production of DO by algae ($r_{DO,\ photo}$). The solubility of oxygen (C* = 7.043 mg/L) was calculated for 15.0 ppt water, 30 °C, at atmospheric pressure [59]. The fish respiration rate was estimated as a constant based on Chandra et al. [60] for catfish. The microbial respiration rate was estimated using U.S. EPA's [61] procedure for specific oxygen uptake rate. The gas transfer (K_L) values were determined empirically based on the nighttime values when DO accumulation was minimal.

Carbon accumulation is summarized by Eq. (4):

$$\frac{VdC(C)}{dt} = m_{C,feed} - m_{C,fish} - m_{C,peri} - m_{benth} \pm QC_{TIC} \pm QC_{DOC} \pm VK_{L,mech}A\left(C^*_{CO2} - C(t)\right) \pm VK_{L,inlet}A\left(C^*_{CO2} - C\ (t)\right) \pm Vr_{DOC} - Vr_{CO2,photo} \pm Vr_{DOC/TIC} \pm Vr_{uptake,DOC} \pm Vr_{uptake,TIC} \quad (4)$$

The total accumulation of carbon mass is described as the product of the volume and the change in the carbon concentration (C(C)). The major solids fractions are for the carbon content of feed, fish, periphyton, and benthic solids. Gas exchange of CO_2 ($\pm K_{L,\ mech}A \pm K_{L,\ inlet}A$) occurs across the surface of the RAS. The solubility of carbon dioxide (C_{CO2}*=0.637 mg/L) was calculated for 15.0 ppt water, 30 °C at atmospheric pressure using the current NOAA concentration for CO_2 and the method of Weiss [62]. Respiration was assumed to produce CO_2 from carbon already in the RAS. The dissolution of dissolved organic feed is

described by r_{DOC}.The dissolved total inorganic carbon (TIC) and dissolved organic carbon (DOC) were significant intermediary factors in carrying nutrients to periphyton, while the uptake of the carbon is described by ($r_{uptake,\ DOC}$,$r_{uptake,\ TIC}$). The reaction between the two (TIC ↔ DOC) is represented by $r_{DOC/TIC}$ and is significant because algae are autotrophic versus most bacteria in the system, which are heterotrophic. The photosynthetic rate $r_{CO2,\ photo}$ was found by simplifying and assuming steady state.

3. Results and discussion

3.1. System startup and fish health

System startup was pivotal in both phases. During the first week of Phase I, only floc forming bacteria and algae were observed on the substratum. After two weeks, algae mats began to attach to the nets. After a month, a true periphyton community developed based on observations. The morphology of the periphyton on the substratum showed the development of a biofilm and green microalgae, which thickened in the second week. Filamentous blue-green algae cells that developed were predominately members of *Oscillatoriaceae*. Additionally, calanoid copepods were consistently observed in the samples. The startup of RAS2 in Phase II was slower. One net from RAS1 was placed in RAS2 as the microbial seed community. During this time, microscopic analysis of RAS2 periphyton confirmed only two common taxa: diatoms and copepods. After three months of switching nets between RAS1 and RAS2, microscopy and daily water quality data were similar in both systems. The taxa broadened to include diatoms, copepods, rotifers, filamentous

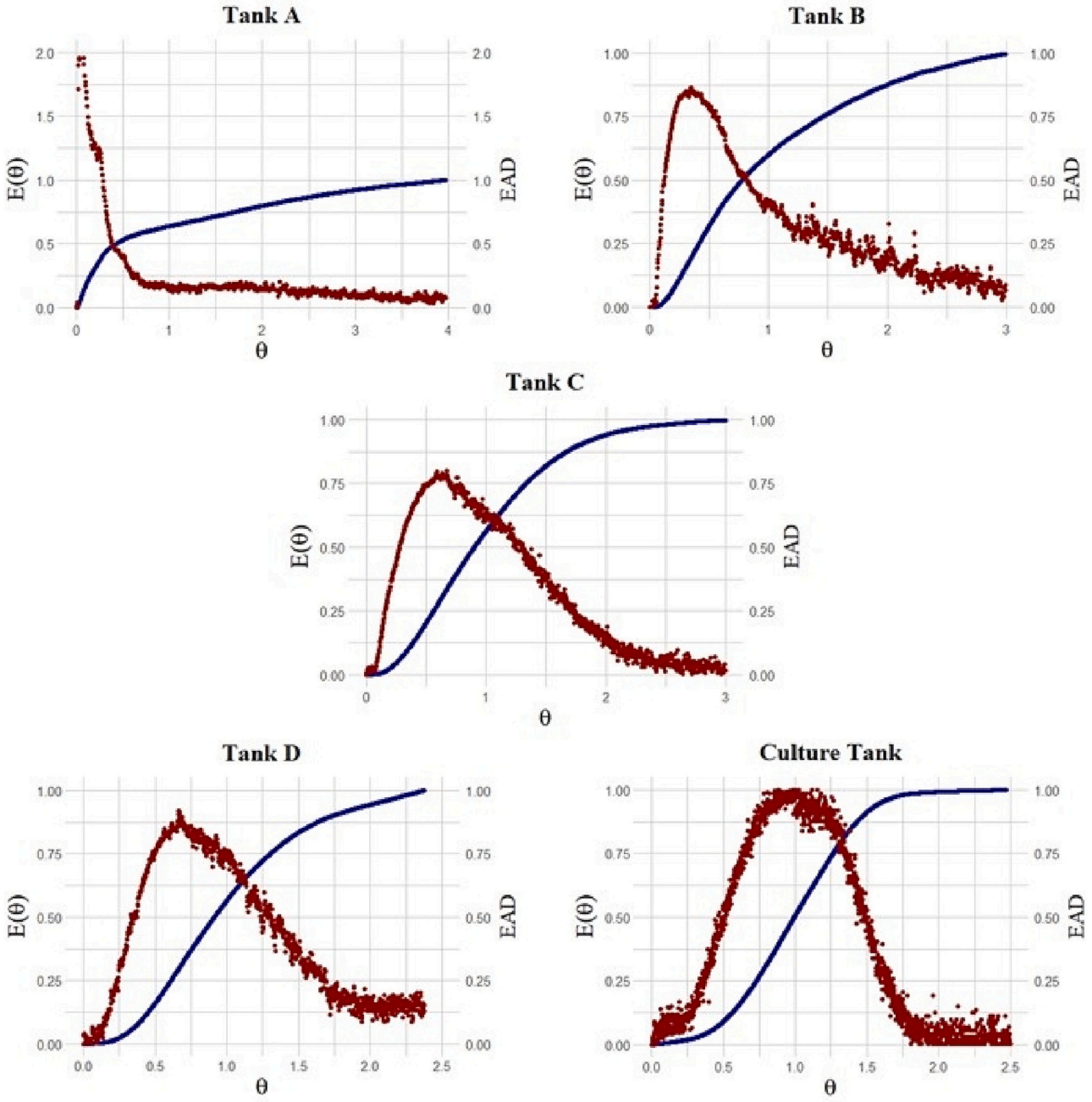

Fig. 2. Residence time distributions (E(θ), red line) and exit age distributions (EAD, blue line) given normalized time and tracer concentrations for the periphyton biofilter and culture tank. Note that the conservative tracer was a premixed concentrated salt solution that was into the inlet distributer in tank A. (For interpretation of the references to colour in this figure legend, the reader is referred to the web version of this article.)

and haptophyte algae in both RAS.

The euryhaline hardhead catfish easily transitioned from full strength saltwater (35 ppt) to brackish water (15 ppt). There was one mortality, due to jumping, between Phases I and II, after which the water level in the culture tank was lowered to prevent future jumpers. Otherwise, there were no recorded mortalities, injuries, or diseases. The SGR for RAS1 catfish was 0.63 ± 0.19 %, while the SGR for RAS2 was 0.78 ± 0.19 %. The FCR in RAS1 was 2.2 ± 0.2 $\frac{kg\ feed\ in}{kg\ fish\ growth}$ while the FCR in RAS2 was 1.8 ± 0.2 $\frac{kg\ feed\ in}{kg\ fish\ growth}$.

3.2. Mass transport

The response of the biofilters and the culture tank to the addition of the conservative tracer was measured separately in each tank (Fig. 2). Based on the tracer study, the fluid moving through tanks A–D had between a 7 to 40 % higher HRT than the theoretical HRT. The deviation from the ideal HRT decreased with increasing tank number. For tank A, the theoretical HRT value was 1.0 h versus the tracer study HRT, which was 1.4 h (40 % greater). For tank D, the theoretical HRT was 4.0 h, while the tracer HRT was 4.3 h (7 % greater). This indicates the presence of hydraulic stagnant zones (or dead zones). In contrast, the culture tank had a theoretical HRT of 6.5 h versus the tracer HRT of 6.1 h (6 % lower). This indicates hydraulic short-circuiting in the culture tank.

The location and causes of the dead zones and short circuiting were further investigated using the OTT MF flow meter and fluorescent dye study. The flow meter showed higher velocities immediately below the inlet distributer and along the edge closest to the outlet ($\vec{v}$ = 2 ± 0.5 cm/s) of the periphyton biofilters, while velocities were non-detectable along most edges of the cuboid tanks. The dye study (at HRT = 1 h) confirmed that the inlet distributer successfully mixed the influent across the biofilter tank in less than 5 min; however, the dye resided for a longer time in regions along the edge of the cuboid tank. The results from the OTT MF and the fluorescent dye indicate that the dispersion through most of the tank occurs due to eddies in the micrometer range. The hydraulic short-circuiting in the culture tank was likely due to the pump location and high recirculation flow rate. Optimally, the pump should be placed at a location further away from the biofilter outlet. In summary, the tracer study showed that the deviation from the theoretical HRT decreased with the number of tanks and that mixing was uniform in the tanks with some exceptions near the edges.

The particle size distribution of the ground feed affected the suspension and settling of nutrients in the RAS. The feed particle size analysis showed a log-linear distribution: 33.6 ± 4.1 % was >600 μm, 43.9 ± 3.6 % was >300 μm, 51.3 ± 3.4 % was >100 μm, 60.4 ± 3.7 % was >35 μm, 76.1 ± 4.0 % was >0.45 μm and the remaining 23.9 ± 4.0 % was dissolved in the aqueous phase. The Stokes' settling velocity for small feed particles (<35 μm) is <1 mm/s [63]. It can then be inferred that approximately 60 ± 4 % of the input feed remained suspended, and depending on the mixing, contacted periphyton nets.

The dispersion of fluid in the reactor was further investigated by evaluating velocity gradient values ($\overline{G}$). The adjusted $\overline{G}$ value was 9.04/s for HRT = 1 h and decreased to 2.3/s for a HRT of 8 h. The $\overline{G}$ value affects mixing, particle sedimentation and transport of particles to the periphyton nets. In relation to sedimentation versus distribution of particles onto the periphyton nets, the mixing was high enough to keep particles >35 μm in suspension (60 % of feed input). $\overline{G}$ values were lower than required for flocculation of insoluble particles [50]. Most of the literature on $\overline{G}$ values are for conventional rapid mixing and flocculation processes; however, the values found in this study may be in the correct range for dispersion of nutrients to periphyton. The lower $\overline{G}$ values may be justified by considering that the primary goal for hydrodynamic mixing is to add just enough energy to evenly distribute feed particles onto the sticky polysaccharide periphyton matrix. In this respect, the inlet distributer was found to be effective, as the dye tracer was homogenously dispersed within the reactor by the inlet distributer. The disadvantages found for this type of inlet distributer were the narrow range of flows and the need for regular cleaning.

Both periphyton biofilters and ATS take nutrients that are carried in a moving flow and repurpose them through an attached growth microbial community. The mass transfer of nutrients to the microbial biofilm is affected by the differences between the two systems, which includes the reactor type, substratum, and land area. Oscillating hydraulic loads and high length/width ratio in ATS approximates a plug flow reactor [48]. In contrast, periphyton biofilter tanks have a lower length/width ratio with a consistent mean HRT to regularly circulate water. The reactor for periphyton biofilters is approximated by a CMFR in series model. Furthermore, Levy et al. [23] showed that vertical net orientation in periphyton biofilters results in higher biomass yields per land surface area.

Prior studies of ATS hydrodynamics showed that both the shape of the media and hydrodynamics affected system performance. Adey et al. [29] applied a structured substratum (basal screen with braided fibers), which increased periphyton growth by 157 %. This indicates that changing the structure of the substratum can increase the transport of nutrients through the boundary layer. For oscillating versus vortex flow, periphyton growth was increased by 21 % for the oscillating flow [30]. Further research is needed to test the application of different structured substratum and oscillating flow patterns on periphyton biofilters.

3.3. Periphyton biomass

Periphyton biomass yield was quantified in Phases I and II using the sample strip procedure described previously. After the periphyton was washed from the HDPE substratum, the biomass was processed for DW, AFDW, and VS (DW minus AFWD). The yields of periphyton production are summarized in Table 2. The average DW was 6.0 ± 0.5 % (n = 4) of the wet weight, while the average VS was 61.7 ± 15.6 % of DW. The general biomass yield trends indicate that the maximum yield was reached on day 18 or 21. The lowest Phase I biomass yield occurred at a HRT of 2 h. The highest biomass yield occurred at a HRT of 4 h. The data indicate that the highest periphyton biomass growth yield occurs at intermediate fluid velocities, where high nutrient flux is achieved, yet excessive sloughing does not occur. Prior limnological studies also showed that periphyton had peak biomass yields at moderate near bed velocities [64]. Unfortunately, there was not a detectable linear trend in biomass yield versus flow rate. Risse-Buhl et al. [65] found that at low nutrient concentrations the variability in periphyton is explained more by environmental and seasonal factors, such as light availability, as compared to hydrodynamic effects. Variations in environmental conditions, such as changes in weather patterns, may have influenced biomass yields to a greater extent than hydrodynamic changes. Pacheco et al. [66] also reported a strong influence of irradiance and nutrient concentration in relation to the effect of flow on periphyton. The growth rate for low profile algae were particularly correlated with flow rate. This supports the results that moderate flow rate is correlated with

Table 2
Phase I dry weights and volatile periphyton yields (g/m^2)[a].

HRT (hours)	Type	Day 11	Day 14	Day 18	Day 21
1	DW	3.4 (0.1)	3.7 (0.7)	8.8 (1.7)	8.2 (0.8)
	VS	1.0 (0.4)	1.9 (0.7)	4.4 (2.2)	5.4 (0.9)
2	DW	1.1 (0.7)	2.3 (0.5)	7.0 (1.2)	4.8 (1.0)
	VS	0.4 (0.7)	1.4 (0.5)	5.2 (1.2)	4.2 (1.0)
4	DW	4.3 (0.6)	4.8 (1.1)	9.0 (2.5)	11 (0.2)
	VS	2.4 (0.6)	3.3 (1.1)	5.6 (2.5)	7.8 (0.3)
6	DW	4.7 (0.3)	2.1 (0.6)	2.4 (1.4)	7.3 (0.9)
	VS	4.6 (0.3)	1.5 (0.6)	0.9 (1.4)	4.7 (0.9)
8	DW	2.0 (0.6)	3.8 (1.3)	6.6 (2.0)	6.6 (1.4)
	VS	1.4 (0.6)	2.0 (1.4)	4.7 (2.0)	3.7 (1.4)

[a] Values in parenthesis represent one standard deviation.

higher biomass yield, although there is high variability at low nutrient concentrations.

Phase II biomass yields (Fig. 3) were approximately three times that of Phase I (HRT = 1 h). The results are consistent with Bothwell's model (1989) for periphyton growth since the feed rate was increased from 35.00 g/day in Phase I to 70.00 g/day in Phase II. The maximum yield for RAS1 (32.3 g DW/m^2) was observed at four weeks, while the maximum yield for RAS2 (27.2 g DW/m^2) was observed at 3 weeks (Fig. 3). A major reason for this difference was that RAS1 had been running for a full year, while RAS2 had only been running for four months. Nguyen [17] observed that the prokaryote community in periphyton was predominately influenced by development and growth over time. The VS/DW ratio in RAS2 (78 ± 4 %) was significantly higher than in RAS1 (72 ± 2 %) ($p = 0.047$), most likely due to changes in the carbon fixation pathways in periphyton [18]. The biomass yield is roughly proportional to the difference in the stocking density between the two studies (3.8 kg/m^3 in this study versus 10–15 kg/m^3 in [12]), indicating that periphyton growth rate is predominately influenced by stocking density. This suggests that the growth rate is predominately influenced by the stocking density.

Sloughing of periphyton biomass was not observed in the normal weekly harvest regime in Phase I or II. This is likely because periphyton adapts to fluid shear as it grows, leading to higher biomass separation during sudden changes [67]. In between phases the periphyton was allowed to age for 6–8 weeks, and the sheet would be thick enough to peal or slough off with hydraulic force or by hand, which eased the harvest procedure considerably.

Optimization of the reactor with respect irradiance is needed to raise the algal portion and to help produce periphyton used to feed the culture species [68]. Light intensity at the surface of the reactors was only 13 ± 2 % (n = 4) of the light outside the greenhouse (1314 versus 175 μmol/m^2s). The light decreased quickly with depth, approximately by one-half for every 10 cm depth [39]. The effect of light inhibition was further observed when after harvesting the periphyton nets, a concave parabolic gradient of green microalgae would often be visible.

This study indicates that the use of the areal loading rate $\left(\frac{Flow*Concentration}{Substratum\ Area}\right)$ as an independent variable to predict periphyton biomass is restricted by biofilter conditions. For instance, at low concentrations, it was found that the biomass is not proportional to velocity and has raised variability. In contrast, the literature suggests that at brief high areal loading rates, periphyton growth rates decrease for an extended period [69]. For future studies, it is recommended that the light and nutrient loading be optimized first followed by the velocity.

Periphyton biofilters, like ATS, remove toxic nitrogen species, add DO, and reclaim nutrients to produce biomass [32]. Besides reactor type and substratum per land area, ATS differ from periphyton biofilters in the lighting, growth rate, and harvest regime. ATS usually have shallow depths and are directly exposed to sunlight. In contrast, net placement in periphyton biofilters allows for a gradient of lighting, decreasing with reactor depth, resulting in lower growth rates [39]. This leads to a periphyton harvesting frequency of approximately once per four months versus optimal ATS harvesting frequency of once per 1–2 weeks [31]. While the growth rates are lower, the gradient of light and modularity of the harvest regime likely encourages a diverse group of algae and phototrophic microbes across the reactor light gradient.

3.4. Water quality analysis

Phase I temperature, salinity, DO, and pH measurements are summarized in Table 3. The salinity stayed the same between trials. Although the average pH fluctuated, the variance and average between trials did not significantly differ ($p > 0.10$). When ranked by order of trial, there was a decrease in the average temperature of 1.25 °C/trial ($R^2 = 0.834$) due to seasonal changes. Because of the influence of temperature on DO, the DO values are represented as percent saturation.

Table 3
Phase I water quality summary.

HRT	Temp C	DO (%)	pH	Salinity (ppt)
1	23.6 (2.7)	79.7 (20.9)	8.14 (0.33)	15.2 (0.3)*
2	28.2 (0.7)	79.7 (14.8)	8.03 (0.21)	15.2 (0.2)
4	27.8 (1.0)	73.5 (14.2)	8.27 (0.27)	15.3 (0.2)
6	29.3 (0.8)	65.6 (45.8)	8.07 (0.25)	15.5 (0.2)
8	27.1 (1.2)	16.1 (7.5)	7.92 (0.26)	15.4 (0.3)

* Standard deviations are shown in parenthesis, n ≥ 6 for each HRT.

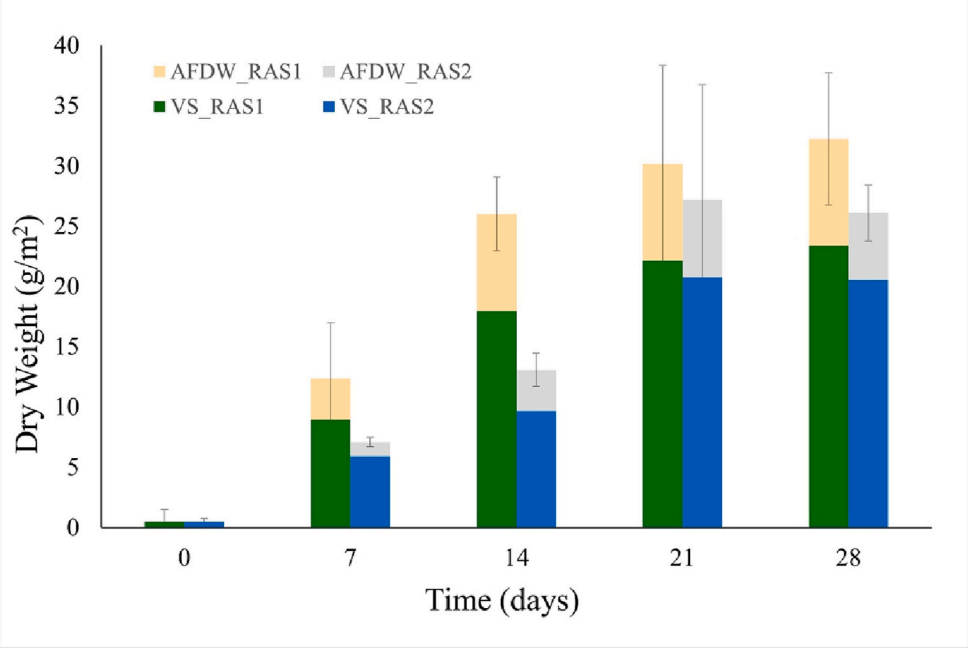

Fig. 3. Phase II periphyton volatile solids (VS) and ash-free dry weight (AFDW) yield for one month using a harvest regime of one tank/week. Error bars show standard deviation for the DW (AFDW+VS).

Phase I DO values (no blower in culture tank) followed a second-degree parabolic trend ($R^2 = 0.962$) as a function of HRT.

$$DO\%(HRT) = -\frac{2.23}{hr^2}\,HRT^2 + \frac{11.8}{hr}\,HRT + 67.4 \quad (5)$$

The change in DO between culture tank influent and effluent provided a way of tracking the loss or generation of DO in the biofilter due to photosynthesis and DO gas efflux (Fig. 4). The change in DO at a HRT of 1 h was 29.9 ± 11.0 %. In contrast, the change in DO at a HRT of 8 h was 104 ± 36 %. This result can be misleading because when the product of flow rate and change in concentration is taken to find the mass flow rate, the biofilters provided 13 mg DO/min at the HRT of 1 h, while only 5.7 mg DO/min was provided at the HRT of 8 h. The lower mass flow of oxygen at a HRT of 8 h indicates either a reduction in DO efflux and/or in the rate of photosynthesis. Note that the culture tank DO at a HRT of 8 h was too low to support fish health. Although the average DO for Phase I at a HRT of 1 h would likely have supported fish health, the variation was too high to safely support fish. Therefore, a coarse bubble diffuser was installed in the culture tank for Phase II.

For the Phase II samples ($n = 12$) measured at 1 pm, there were no significant differences between RAS1 and RAS2 in terms of pH (RAS1 pH = 7.97 ± 0.12, RAS2 pH = 7.94 ± 0.11), DO (RAS1 DO = 95.1 ± 8.0 %, RAS2 DO = 99.2 ± 10.8 %) or salinity (RAS1 salinity = 15.3 ± 0.4 ppt, RAS2 salinity = 14.6 ± 1.2 ppt). There were significant differences in temperature between the two systems (RAS1 27.5 ± 0.6 °C, RAS2 28.2 ± 0.7 °C), probably due to a higher fan airflow rate over RAS1. There were also significant differences in DO levels between Phase I at a HRT of 1 h and Phase II, which was operated at 1 h ($p = 0.015$), due to the inclusion of the coarse bubble diffuser system during Phase II.

The effect of HRT on inorganic nitrogen species removal rates during Phase I was substantial (Table 4 and Table S1). Note that the first trial run was conducted at a HRT of 6 h, and different nitrogen removal patterns were observed at HRT = 6 h than in the rest of the trials, most likely due to acclimation of microbial populations. Although some NO_2^- accumulation was observed, average NO_2^- concentrations were <1 mg NO_2^--N/L, with a maximum of 2.2 mg NO_2^--N/L at a HRT of 2 h, which is well below the toxic level for fish (Table 1). The removal of TIN and non-detection of nitrate at a HRT of 6 h reveals that there was a transformation pathway from nitrite to either periphyton biomass or to nitrogen gas via denitritation. The higher flow rate at a HRT of 2 h likely changed periphyton to favor NO_2^- oxidizing bacteria by carrying a greater nitrogen mass and raising the DO generation rate [70], therefore leading to conventional nitrification/denitrification at the other HRTs.

TAN was removed at about the same rate for all the trials (Table 4). The effluent TAN from the biofilter was <0.2 mg NH_4^+-N/L for all trials, well within the safe level for fish health (Table 1). Differences between biofilter influent and effluent TAN concentrations (Fig. 5) significantly increased with increasing HRT ($p < 0.01$). At a HRT of 8 h TAN accumulated in the culture tank because the mass flow rate of TAN out of the culture tank was lower than the daily addition of feed and nutrients. Considering the importance of TAN toxicity on fish health, Fig. 5 indicates that the safest HRT was 1 h. NO_3^- was generated in most trials, although the concentrations stayed below 30 mg NO_3^--N/L for all trials and phases. Overall, the TIN removal was inversely correlated with HRT ($R^2 = 0.81$), indicating increased transport due to dispersion. Variations in TIN during Phase II were due to fluctuating NO_3^- concentrations (see Table S1). After the end of Phase II, the fish and feeding regime in RAS1 remained the same and NO_3^- accumulation was not observed, but rather stayed at values close to 20 NO_3^--N mg/L.

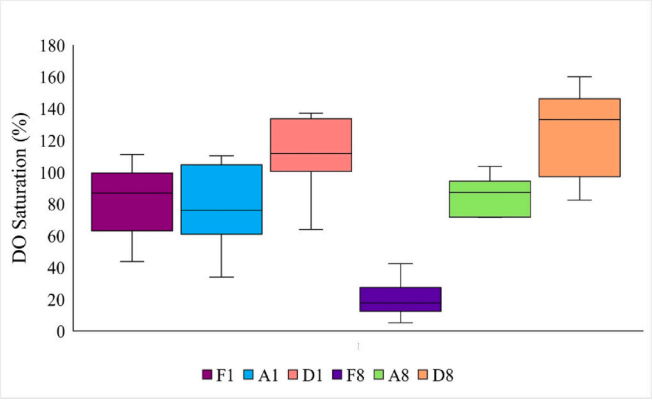

Fig. 4. Phase I DO levels in the fish tank (F), tank A (A), and tank D (D) for two different HRTs (HRT 8 h: F8, A8, D8, and HRT 1 h: F1, A1, D1) as an average of measurements in Phase I (n = 7 for HRT of 8 h, n = 10 for HRT of 1 h).

Table 4
Removal rates of inorganic nitrogen species at daytime (13:00)[a].

	NO_2^- - N mg/min	NO_3^- - N mg/min	TAN - N mg/min	TIN - N mg/min
Phase I				
1	0.46 (0.42)	0.03 (0.96)	1.02 (0.96)	1.11 (0.91)
2	0.19 (1.99)	−0.39 (1.92)	0.87 (1.15)	0.65 (2.24)
4	0.75 (0.31)	−1.17 (0.52)	1.00 (0.63)	0.68 (0.69)
6	−0.08 (0.09)	0.50 (0.31)	0.27 (0.25)	0.39 (0.52)
8	0.63 (0.37)	−1.38 (0.85)	1.06 (1.10)	0.31 (1.07)
Phase II				
RAS1	0.25 (0.13)	−0.76 (6.83)	nd	−0.51 (6.89)
RAS2	0.63 (0.19)	−0.93 (6.18)	nd	−0.30 (6.24)

[a] Calculated by taking the difference in concentration between biofilter influent and effluent and multiplying by the flow rate. Negative values indicate generation. One standard deviation is given in parenthesis, "nd" stands for non-detect.

The CO_2 concentration in the biofilter was barely detectable, with a constant value dissolved in the liquid phase. CO_2 measurements were either 0 or 1 mg/L (n = 5), which was at the minimum detection limit of the Oxyguard meter and close to the saturation level C*. Neither was there a difference in the inorganic carbon fraction as measured between the culture tank and biofilter for RAS1 or RAS2. The total alkalinity stayed at 142 ± 17 mg/L as $CaCO_3$ (n = 13). The results indicate that the algae were quickly exhausting the dissolved carbon dioxide. Iwan Jones et al. [35] reported that periphyton can reduce the dissolved carbon dioxide concentration to <0.024 mg/L. The CO_2 measured stayed far below the toxicity level required to keep healthy fish (Table 1).

In summary, during Phase I there were significant differences in DO, TAN, and NO_2^-/NO_3^- concentrations as a function of HRT. Results were somewhat confounded by temperature changes at a rate of −1.25 °C/trial due to seasonality. DO saturation was found to follow a 2nd order polynomial relationship with HRT. TAN accumulation occurred in the culture tank when the RAS was operated at long HRTs. No significant differences were observed between Phase II RAS1 and RAS2 for salinity, pH, or DO, although there was a small (<1 °C) difference in temperature. Dissolved CO_2 was detected at 1 mg/L or less. The removal rates for nitrite and TAN were normalized to units of N/(L*m^2*day) and listed in Table S3.

3.5. Mass balances

The DO mass balance was influenced by diel cycles; DO would rise above 100 % saturation during the day and fall below saturation during night (Fig. 6). With the blower running at night, the minimum DO concentration was found to occur at 22:21. Light was available as detectable PAR between 6:51 to 20:05 (Table S2). The normal curve for the period of DO production corresponds to the normal curve for irradiance. The average daily PAR flux into the biofilter was 7.6 ± 1.0 mols/m^2. The days where the blower was not operated during daytime hours (days 6 to 10 in Fig. 6) also indicated a higher degree of variation in DO.

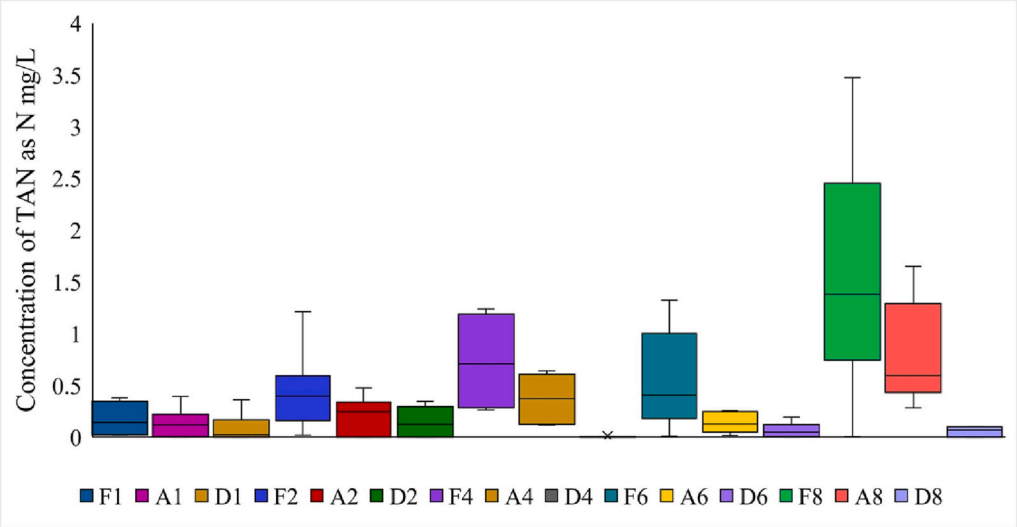

Fig. 5. Total ammonia nitrogen (n ≥ 6 per box) concentrations for the fish culture tank (F), tank A, and tank D. The second character represents the HRT (e.g., A1 is tank A at HRT = 1 h).

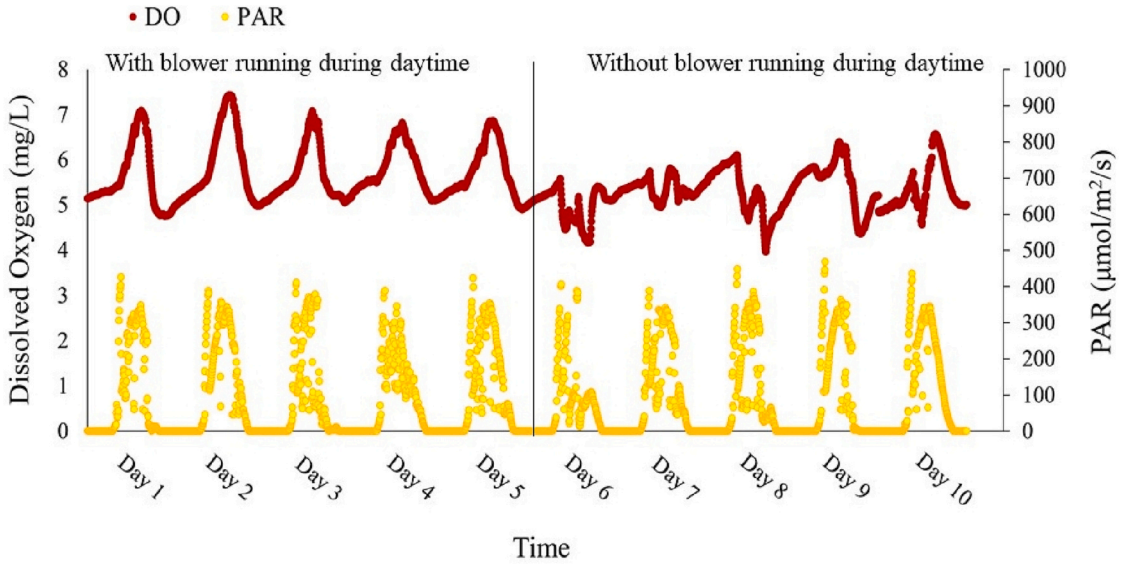

Fig. 6. Phase II DO concentrations as related to the availability of sunlight (HRT = 1 h). Photosynthetically active radiation (PAR) is the irradiance measured in the light range between wavelength of 400 to 700 nm. During the first five days the blower was running constantly. During days six to ten the blower was running only at night (5 pm to 9 am).

The changes could also have been due to shifts in prokaryote/algae kinetics [57].

Several assumptions were made for the DO mass balance regarding boundary conditions and time due to the experimental setup and data collection. The boundary was redrawn around the culture tank (Fig. 1) where the HACH sensor was placed. Fick's law diffusion of DO in the tank was assumed to take place rapidly over a time much lower than each DO measurement. The rate of photosynthetic DO production was considered equal to the difference between the mass flow in and out of the culture tank. The fish and microbial respiration rate were found to be non-linear starting in the mid-afternoon (14:14) because of the daily input of feed. Therefore, the time at which the mass balance was performed was limited to the daytime hours and the time that DO was positively accumulating in the culture tank (from 6:50 in the morning to 14:14). The volumes (Fig. 1) were associated with the location in the RAS that the reaction occurred. Thus, for total accumulation as measured by the HACH meter, the culture tank volume was used, for photosynthetic production, the biofilter volume was used, for the total transfer of gas and total respiration, the entire RAS volume was used.

DO accumulation, gas transfer, respiration, and photosynthetic

Table 5
Mass balances for DO during daytime (6:50 to 14:14)[a].

Day	$V_C \sum \frac{dC(DO)}{dt}$	$V_{RAS} \sum K_{L,g} A(C_{DO}^* - C(t))$	$V_{RAS} \sum r_{DO,resp}$	$V_B \sum r_{DO,photo}$
1	8.662	4.945	−14.91	18.62
2	9.978	1.774	−14.91	23.11
3	6.966	4.308	−14.91	17.57
4	5.854	4.678	−14.91	16.08
5	7.028	5.185	−14.91	16.75
Average	7.698	4.178	−14.91	18.43
SD	1.621	1.383	-	2.785

[a] Units for all summations are in dissolved oxygen (DO g/day) for the culture tank.

Table 6
Summary of nitrogen mass balance.

	$m_{N,\ feed}$	$m_{N,\ fish}$	$m_{N,\ peri}$	$m_{N,\ TS}$	$QC_{N,\ TIN}$	r_{denit}
Mass N (g/d)	4.54 (0.02)	1.72 (0.26)	0.54 (0.02)	1.5 (0.6)	0.29 (0.03)	0.5 (0.6)
Approx. %	100 (0.44)	37.8 (5.7)	12 (0.4)	33 (13)	6.4 (0.7)	11 (13)

production are listed for five Phase II sample days in Table 5. Microbial uptake of DO was found to be 1.593 ± 0.077 mg DO/(L*h) for 1 g of benthic solids. The two-film gas transport value was found to be $K_{L,\ g}A$ = 0.49 ± 0.15/h. Extrapolating the $K_{L,\ g}A$ from Chern and Yang [71] considering depth, coarse diffusion, and airflow rate also gives a $K_{L,\ g}A$ between 0.3 and 0.8/h. The average DO input due to the blower during the nighttime (22.74 ± 1.06 g/d) was much greater than the calculated input during the day (4.178 ± 1.383 g/d). This occurred because of the greater difference between saturation C_{DO}* and C (t) that occurs at night versus the day, where photosynthesis can support much of the RAS needs. There was a period from about 11:00 to 15:30 where the blower transferred DO out of the reactor because the culture tank concentration exceeded C_{DO}*. The mass transfer of DO to the culture tank due to the photosynthetic biofilter was found to average 18.43 ± 2.79 mg/L/day.

The mass balance revealed that photosynthetic activity of the periphyton can directly provide DO to the culture tank to help support fish life. The DO mass balance results, when combined with DO generation data at varying HRT (Fig. 4) indicated that the highest flow rate tested (HRT 1 h) was best for maintaining DO in culture tank. The literature supports the fact that the photosynthetic production of DO is related to flow rate, with intermediate flows supporting greater DO production than either stagnant water or high flow rates [70]. In contrast to the assumptions, the respiration term changes due to the circadian rhythm of the fish and the availability of food for microbes. Therefore, the DO production rate of 1.31 ± 0.20 mg/(L*m^2*day) is likely to be an intermediate value (Table 5 adjusted for net SA).

The settleable solids (TS = 30 % in this study) indicated a nitrogen sink that, according to Boxman et al. [19], can be repurposed as fertilizer. Compared to N mass balance in an IMTA using halophytes for N, periphyton (excluding filamentous algae) removed 12 % N as feed compared to 6 % N found for plant removal [4]. This indicates periphyton's versatility to biosynthesize different TIN species and simple DON compounds, such as urea [58]. The denitrification rate (4.3 %) is lower than the 17 % removal found by Boxman et al. [19] utilizing a slow sand filter in an IMTA system. This may be due to the relatively high harvest frequency used in this study, because a thin layer of periphyton has lower potential for development of anoxic zones than a thick periphyton layer.

Biosynthesis of nitrogen by the extractive species is one of the key advantages of IMTA systems due to the ability to recover nutrients not taken up by the culture species (extractive N or C) and reduction of nutrient discharges to the environment. Nitrogen processed by the catfish was found to be 37.8 % of the daily feed (Table 6). This left 62.2 % of feed input (2.82 g N/day) nitrogen available as an N source to algae and microbes. A sizeable portion of the waste (0.37 ± 0.07 g N/day or 8.1 % feed) was due to the fast-growing filamentous algae that were operationally removed from the top of the reactor. Periphyton took up 0.54 g N/day or 12 % of feed. If a purpose could be found for the filamentous algae, then a significant additional IMTA product would be created. Between the operationally removed filamentous algae and the harvested periphyton, a total of 32 ± 4 % of extractive N was recovered.

The major species measured for the carbon mass balance included the solid fractions and the photosynthetic portion (Table 7). CO_2 was detected near saturation (§3.4), therefore the transport of CO_2 gas in and out of the RAS was neglected. TIC was only detected at a constant level which was speciated between H_2CO_3 at 4.7 mg/L, HCO_3^- at 282.6 mg/L, and CO_3^{2-} at 3.0 mg/L [56]. The terms for reaction and mass transport of TIC and DOC were considered intermediary, although it is recommended that future investigations include these terms. The most likely

Table 7
Summary of carbon mass balance.

	$m_{C,\ feed}$	$m_{C,\ fish}$	$m_{C,\ peri}$	$m_{C,\ TS}$	$r_{CO2,\ photo}$
Mass C (g/d)	61.5 (0.1)	19.8 (0.7)	10.6 (0.6)	16.2 (0.2)	15.0 (0.7)
Approximate %	100 (0.2)	32.2 (1.1)	17.2 (1.1)	26.3 (0.4)	24.4 (1.1)

pathway taken by carbon was as small organic particles transferred to periphyton as studied by the $\overline{G}$ values and feed gradation curve (§3.2). Boxman [4] reported hydrolysis of small carbon particles in an IMTA sand filter as well as removal of organics (as measured by chemical oxygen demand) in plant bed influent versus effluent. The fish took up the largest fraction of the carbon (32.2 %), followed by solids that settled to the benthic zone (26.3 %). The portion not eaten by fish was 41.7 g C/day or 67.8 % of feed input. Periphyton also took up a sizeable fraction (17.2 %). The fate of the carbon reclaimed from photosynthesis (24.4 %) was assumed to be equal to the mass of *Oscillatoriaceae* that was produced. In total, filamentous algae and periphyton recovered 61.4 ± 2.2 % of extractive C.

This study showed that the HRT is a significant factor in mass balance due to changes in DO, nutrient kinetics, and periphyton growth. The lower HRTs encouraged high DO which provided advantages to high trophic level organisms such as copepods and fish. In addition, the lower HRTs raised the aqueous nutrient dispersion and removal rate for TIN. On the other hand, the higher HRTs allowed for easier control of denitrification. Periphyton growth was found to prefer the intermediate HRTs.

In summary, periphyton were found to take up nutrients through several pathways, by biosynthesis, fueling reactions (nitrification, denitrification, respiration) and by hydrolysis (ammonification). The reaction rates are summarized in the supplementary materials (Table S3). The mass balance on DO indicates that periphyton produced 1.31 ± 0.20 DO mg/(L*m^2*day) during daytime hours, which was almost enough to support fish biomass without the use of a blower. The mass balance on nitrogen showed that 37.8 ± 5.7 % of N ended up as fish and of the remaining N, 32 ± 4 % was recovered as periphyton or *Oscillatoriaceae*. The carbon mass balance showed that 32.2 ± 1.1 % of C ended up as fish and of the remaining C, 61.4 ± 2.2 % was recovered as periphyton or *Oscillatoriaceae*.

4. Conclusions

In this study, we designed, constructed, and operated brackish RAS with integrated periphyton biofilters. The effects of hydrodynamics on nutrient mass transport, periphyton biomass growth, water quality, and mass balances of C, N, and DO were investigated. System startup took 2–4 months for both RAS, with the microbial community beginning as a biofilm and then broadening to include Haptophytes, *Oscillatoriaceae*, diatoms, calanoid copepods, and other microbes.

Recirculation flow rates through the four-tank biofilter were varied to determine the effect on mass transport and periphyton growth rates. Tracer tests revealed that there was a 7 % deviation (HRT 1 h) between experimental and theoretical HRT due to the presence of hydraulic dead zones along the edge of the tanks. The reactor type was close to an ideal CMFR tanks in series model. Mixing was found to be homogenous even at low velocity gradient values. Optimal periphyton growth requires the transport of nutrients by diffusion or dispersion; however, the flow cannot be so high that it promotes premature biomass sloughing. An

intermediate flow rate resulted in the greatest biomass growth in Phase I. Phase II growth rates were higher than Phase I, due to the higher nutrient inputs caused by higher fish stocking densities. Sloughing of excess periphyton biomass was minimal.

Nutrient and water quality results were used to elucidate the effect of HRT on DO, N, and C balances. At all HRTs, TAN concentrations remained below 0.11 mg/L in the biofilter effluent. Nitrite was also removed from the system and stayed well below toxic levels at all HRTs. DO production increased with decreasing HRT, while nitrate was removed at longer HRTs, which favored denitrification. CO_2 was only detected at 1 mg/L or less. Periphyton and filamentous algae assimilated 32 ± 4 % of extractive N and 61.4 ± 2.2 % of extractive C. The extracted periphyton and filamentous algae product have applications, such as for fish feed, algal oil, biofuel or biochar. Fish and periphyton were found to be a symbiotic IMTA pairing.

CRediT authorship contribution statement

Adam N. Bell: Conceptualization, Methodology, Design, Construction, Analysis, Writing – Original Draft.

Lior Guttman: Conceptualization, Writing – Review and Editing.

Kevan L. Main: Funding acquisition, Conceptualization, Writing – Review and Editing.

Michael Nystrom: Design, Construction.

Nathan P. Brennan: Methodology, Writing – Review and Editing.

Sarina J. Ergas: Funding acquisition, Conceptualization, Methodology, Analysis, Writing – Review and Editing.

Declaration of competing interest

The authors declare the following financial interests/personal relationships which may be considered as potential competing interests: Sarina Ergas reports financial support was provided by US Department of Education. Kevan Main reports financial support was provided by United States Israel Binational Agricultural Research and Development Fund. Adam Bell reports financial support was provided by National Science Foundation.

Data availability

Data will be made available on request.

Acknowledgments

This work has been supported by grants from the National Science Foundation (1735320: Collaborative Research: NRT-INFEWS: Systems Training for Research ON Geography-based Coastal Food Energy Water Systems); the Israel-US Binational Agricultural Research and Development (BARD Research Grant No. IS-5479-22C); and the U.S. Department of Education Graduate Assistance in Areas of National Need (GAANN) program (grant P200A180047). Any opinions, findings, and conclusions or recommendations expressed in this material are those of the author(s) and do not necessarily reflect the views of the funder. Special thanks to Nicole Rhody, Ron Hans, and Evan Worden of Mote Marine Laboratory for their assistance with this research.

Appendix A. Supplementary data

Supplementary data to this article can be found online at https://doi.org/10.1016/j.algal.2023.103028.

References

[1] M. Badiola, O.C. Basurko, R. Piedrahita, P. Hundley, D. Mendiola, Energy use in recirculating aquaculture systems (RAS): a review, Aquac. Eng. 81 (November 2017) (2018) 57–70, https://doi.org/10.1016/j.aquaeng.2018.03.003.

[2] R. Ghamkhar, S.E. Boxman, K.L. Main, Q. Zhang, M.A. Trotz, A. Hicks, Life cycle assessment of aquaculture systems: does burden shifting occur with an increase in production intensity? Aquac. Eng. 92 (August 2020) (2021), 102130 https://doi.org/10.1016/j.aquaeng.2020.102130.

[3] Timmons, Ebeling, Wheaton, Summerfet, Vinci, Recirculating Aquaculture Systems, (2nd ed.), Northeasten Regional Aquaculture Center, Ithaca, NY, 2002.

[4] S.E. Boxman, in: Resource Recovery Through Halophyte Production in Marine Aquaponics: An Evaluation of the Nutrient Cycling and the Environmental Sustainability of Aquaponics 2015, 2015, pp. 1–239. https://digitalcommons.usf.edu/etd/5915/.

[5] T. Chopin, M. Troell, G.K. Reid, D. Knowler, S.M.C. Robinson, A. Neori, A. H. Buschmann, S. Pang, Integrated Multi-Trophic Aquaculture Part II. Increasing IMTA Adoption. Advocate. https://www.globalseafood.org/advocate/integrated-multi-trophic-aquaculture-part-2/, 2010.

[6] M. Asaduzzaman, M.A. Wahab, M.C.J. Verdegem, R.K. Adhikary, S.M.S. Rahman, M.E. Azim, J.A.J. Verreth, Effects of carbohydrate source for maintaining a high C: N ratio and fish driven re-suspension on pond ecology and production in periphyton-based freshwater prawn culture systems, Aquaculture 301 (1–4) (2010) 37–46, https://doi.org/10.1016/j.aquaculture.2010.01.025.

[7] F.S. David, D.C. Proença, W.C. Valenti, Phosphorus budget in integrated multitrophic aquaculture systems with Nile tilapia, Oreochromis niloticus, and Amazon River prawn, Macrobrachium amazonicum, J. World Aquacult. Soc. 48 (3) (2017) 402–414, https://doi.org/10.1111/jwas.12404.

[8] L. Guttman, Periphyton for biofiltration and fish feeding in an integrated multi-trophic aquaculture system: a case study in the Gulf of Aqaba, J. Environ. Soil Sci. 3 (2019) 413–418, https://doi.org/10.32474/OAJESS.2019.03.000171.

[9] ASTM, STP 690 Periphyton Measurements and Applications, in: R.L. Weitzel (Ed.), Methods and Measurements of Periphyton Communities: A Review, 1979, https://doi.org/10.1520/stp35061s.

[10] B. Gangadhara, P. Keshavanath, Planktonic and biochemical composition of periphyton grown on some biodegradable and non-degradable substrates, Journal of Applied Aquaculture 20 (3) (2008) 213–232, https://doi.org/10.1080/10454430802329762.

[11] S.K. Saikia, D.N. Das, Sustainable aquaculture: agro-ecological role of periphyton in ricefish farming, Rev. Aquac. 7 (3) (2015) 172–186, https://doi.org/10.1111/raq.12062.

[12] L. Guttman, A. Neori, S.E. Boxman, R. Barkan, B. Shahar, A.M. Tarnecki, N. P. Brennan, K.L. Main, M. Shpigel, An integrated ulva-periphyton biofilter for mariculture effluents: multiple nitrogen removal kinetics, Algal Res. 42 (June) (2019), 101586, https://doi.org/10.1016/j.algal.2019.101586.

[13] A. Milstein, A. Levy, A. Neori, S. Harpaz, M. Shpigel, L. Guttman, Water quality, ecological processes and management procedures in a periphyton biofiltration system in mariculture: a statistical analysis, Aquac. Res. 49 (4) (2018) 1491–1503, https://doi.org/10.1111/are.13604.

[14] B. Shahar, L. Guttman, Integrated biofilters with ulva and periphyton to improve nitrogen removal from mariculture effluent, Aquaculture 532 (October 2020) (2021), 736011, https://doi.org/10.1016/j.aquaculture.2020.736011.

[15] M.R. Badger, D. Hanson, G.D. Price, Evolution and diversity of CO2 concentrating mechanisms in cyanobacteria, Funct. Plant Biol. 29 (2–3) (2002) 161–173, https://doi.org/10.1071/pp01213.

[16] L. Guttman, S.E. Boxman, R. Barkan, A. Neori, M. Shpigel, Combinations of ulva and periphyton as biofilters for both ammonia and nitrate in mariculture fishpond effluents, Algal Res. 34 (August) (2018) 235–243, https://doi.org/10.1016/j.algal.2018.08.002.

[17] D. Nguyen, Microbial succession in marine periphyton: One step closer to understanding the health aspect of a cost-effective biofilter from an IMTA system, in: 2nd Webinar on Aquaculture and Fisheries, November, 2020. https://crgconferences.com/conference-admin/uploads/aqua_26/1604688677.pdf.

[18] K. Sanli, J. Bengtsson-Palme, R. Henrik Nilsson, E. Kristiansson, M.A. Rosenblad, H. Blanck, K.M. Eriksson, Metagenomic sequencing of marine periphyton: taxonomic and functional insights into biofilm communities, Front. Microbiol. 6 (OCT) (2015) 1–14, https://doi.org/10.3389/fmicb.2015.01192.

[19] S.E. Boxman, M. Nystrom, S.J. Ergas, K.L. Main, M.A. Trotz, Evaluation of water treatment capacity, nutrient cycling, and biomass production in a marine aquaponic system, Ecol. Eng. 120 (June 2017) (2018) 299–310, https://doi.org/10.1016/j.ecoleng.2018.06.003.

[20] O. Dvir, J. Van Rijn, A. Neori, Nitrogen transformations and factors leading to nitrite accumulation in a hypertrophic marine fish culture system, Mar. Ecol. Prog. Ser. 181 (June 2015) (1999) 97–106, https://doi.org/10.3354/meps181097.

[21] G. Savonitto, R. Barkan, S. Harpaz, A. Neori, H. Chernova, A. Terlizzi, L. Guttman, Fishmeal replacement by periphyton reduces the fish in fish out ratio and alimentation cost in gilthead sea bream Sparus aurata, Sci. Rep. 11 (1) (2021) 1–10, https://doi.org/10.1038/s41598-021-00466-5.

[22] D. Davis, A. Morão, J.K. Johnson, L. Shen, Life cycle assessment of heterotrophic algae omega-3, Algal Res. 60 (October) (2021), https://doi.org/10.1016/j.algal.2021.102494.

[23] A. Levy, A. Milstein, A. Neori, S. Harpaz, M. Shpigel, L. Guttman, Marine periphyton biofilters in mariculture effluents: nutrient uptake and biomass development, Aquaculture 473 (2017) 513–520, https://doi.org/10.1016/j.aquaculture.2017.03.018.

[24] R.S. Cottrell, J.L. Blanchard, B.S. Halpern, M. Metian, H.E. Froehlich, Global adoption of novel aquaculture feeds could substantially reduce forage fish demand by 2030. Nature Food. https://www.nature.com/articles/s43016-020-0078-x, 2020.

[25] M. Tsarpali, N. Arora, J.N. Kuhn, G.P. Philippidis, Lipid-extracted algae as a source of biomaterials for algae biorefineries, Algal Res. 57 (May) (2021), 102354, https://doi.org/10.1016/j.algal.2021.102354.

[26] D. Reinecke, L.-S. Bischoff, V. Klassen, O. Blifernez-Klassen, P. Grimm, O. Kruse, H. Klose, U. Schurr, Nutrient recovery from wastewaters by algal biofilm for fertilizer production part 1: case study on the techno-economical aspects at pilot-scale, Sep. Purif. Technol. 305 (October 2022) (2023), 122471, https://doi.org/10.1016/j.seppur.2022.122471.

[27] S. Kim, C. Quiroz-Arita, E.A. Monroe, A. Siccardi, J. Mitchell, N. Huysman, R. W. Davis, Application of attached algae flow-ways for coupling biomass production with the utilization of dilute non-point source nutrients in the Upper Laguna Madre, TX, Water Research 191 (2021) 116816, https://doi.org/10.1016/j.watres.2021.116816.

[28] W.H. Adey, C. Luckett, M. Smith, Purification of industrially contaminated groundwaters using controlled ecosystems, Ecol. Eng. 7 (3) (1996) 191–212, https://doi.org/10.1016/0925-8574(96)00008-0.

[29] W.H. Adey, H.D. Laughinghouse, J.B. Miller, L.A.C. Hayek, J.G. Thompson, S. Bertman, K. Hampel, S. Puvanendran, Algal turf scrubber (ATS) floways on the Great Wicomico River, Chesapeake Bay: productivity, algal community structure, substrate and chemistry1, J. Phycol. 49 (3) (2013) 489–501, https://doi.org/10.1111/jpy.12056.

[30] R.C. Carpenter, J.M. Hackney, W.H. Adey, Measurements of primary productivity and nitrogenase activity of coral reef algae in a chamber incorporating oscillatory flow, Limnol. Oceanogr. 36 (1) (1991) 40–49, https://doi.org/10.4319/lo.1991.36.1.0040.

[31] B. Siville, W.J. Boeing, Optimization of algal turf scrubber (ATS) technology through targeted harvest rate, Bioresour. Technol. Rep. 9 (December 2019) (2020), 100360, https://doi.org/10.1016/j.biteb.2019.100360.

[32] W.H. Adey, K. Loveland, Water quality management with solar energy capture, in: Dynamic Aquaria: Building Living Ecosystems, Academic Press, 2007, https://doi.org/10.1016/b978-012370641-6/50006-6.

[33] A.R. Freeze, J.A. Cherry, in: C. Brenn, K. McNeily (Eds.), Groundwater, Prentice-Hall, Hoboken, NJ, 1979.

[34] M. Holtappels, A. Lorke, Estimating turbulent diffusion in a benthic boundary layer, Limnol. Oceanogr. Methods 2005 (2011) 29–41, https://doi.org/10.4319/lom.2011.9.29.

[35] J. Iwan Jones, J.W. Eaton, K. Hardwick, The influence of periphyton on boundary layer conditions: a pH microelectrode investigation, Aquat. Bot. 67 (3) (2000) 191–206, https://doi.org/10.1016/S0304-3770(00)00089-9.

[36] M.L. Bothwell, Phosphorus-limited growth dynamics of lotic periphytic diatom communities: areal biomass and cellular growth rate responses, Can. J. Fish. Aquat. Sci. 46 (8) (1989) 1293–1301, https://doi.org/10.1139/f89-166.

[37] R. Jan Stevenson, R. Glover, Effects of algal density and current on ion transport through periphyton communities, Limnol. Oceanogr. 38 (6) (1993) 1276–1281, https://doi.org/10.4319/lo.1993.38.6.1276.

[38] D.L. Sutherland, J. Burke, P.J. Ralph, Increased harvest frequency improves biomass yields and nutrient removal on a filamentous algae nutrient scrubber, Algal Res. 51 (September) (2020), 102073, https://doi.org/10.1016/j.algal.2020.102073.

[39] L. Guttman, K. Main, N. Brennan, A. Tarnecki, M. Shpigel, The Use of Plant Based Biofilters to Create Sustainable Mariculture Systems. United States - Israel Binational Agricultural Research and Development Fund (BARD) Grants No. IS 4995 17R. Final Report, 2021. June 2021, 34 pages.

[40] M. Abdel-Tawwab, M.N. Monier, S.H. Hoseinifar, C. Faggio, Fish response to hypoxia stress: growth, physiological, and immunological biomarkers, Fish Physiol. Biochem. 45 (3) (2019) 997–1013, https://doi.org/10.1007/s10695-019-00614-9.

[41] D.J. Randall, T.K.N. Tsui, Ammonia toxicity in fish, Mar. Pollut. Bull. (2002), https://doi.org/10.1016/s1095-6433(99)90247-7.

[42] H. Kroupova, J. Machova, Z. Svobodova, Nitrite influence on fish: a review, Vet. Med. 50 (11) (2005) 461–471, https://doi.org/10.17221/5650-VETMED.

[43] R.H. Pierce, J.M. Weeks, J.M. Prappas, Nitrate toxicity to five species of marine fish, J. World Aquacult. Soc. 24 (1) (1993) 105–107, https://doi.org/10.1111/j.1749-7345.1993.tb00156.x.

[44] A. Ishimatsu, M. Hayashi, K.S. Lee, T. Kikkawa, J. Kita, Physiological effects on fishes in a high-CO2 world, J. Geophys. Res. C Oceans 110 (9) (2005) 1–8, https://doi.org/10.1029/2004JC002564.

[45] W.A. Wurts, R.M. Durborow, Interactions of pH, Carbon Dioxide, Alkalinity and Hardness in Fish Ponds, Issue 464 0, Southern Regional Aquaculture Center, Stoneville, MS, 1992, https://srac.tamu.edu/fact-sheets/serve/112.

[46] L. Rodriguez-Gonzalez, S.L. Pettit, W. Zhao, J.T. Michaels, J.N. Kuhn, N. A. Alcantar, S.J. Ergas, Oxidation of off flavor compounds in recirculating aquaculture systems using UV-TiO2 photocatalysis, Aquaculture 502 (December 2018) (2019) 32–39, https://doi.org/10.1016/j.aquaculture.2018.12.022.

[47] D. Calkins, T. Dunne, A salt tracing method for measuring channel velocities in small mountain streams, J. Hydrol. 11 (4) (1970) 379–392, https://doi.org/10.1016/0022-1694(70)90003-X.

[48] Crittenden, Trussel, Hand, Howe, Tchobanoglous, Borchardt, MWH's Water Treatment Principles and Design, Wiley, New York City, NY, 2012, https://doi.org/10.1002/9781118131473.

[49] J.L. Cleasby, S.W. Freese, Is velocity gradient a valid turbulent flocculation parameter? Natl. Conf. Environ. Eng. 110 (5) (1983) 811–852, https://doi.org/10.1061/(asce)0733-9372(1984)110:5(875).

[50] Y.S. Vadasarukkai, G.A. Gagnon, Influence of the mixing energy consumption affecting coagulation and floc aggregation, Environ. Sci. Technol. 51 (6) (2017) 3480–3489, https://doi.org/10.1021/acs.est.6b06281.

[51] APHA, Standard methods: for the examination of water and wastewater, in: American Public Health Association American Water Works Association Water Environment F, 2017, https://doi.org/10.1016/0003-2697(90)90598-4.

[52] R.M. Carlson, Continuous flow reduction of nitrate to ammonia with granular zinc, Anal. Chem. 58 (7) (1986) 1590–1591, https://doi.org/10.1021/ac00298a077.

[53] ASTM, in: Standard Test Method for Nitrogen in Liquid Hydrocarbons, Petroleum and Petroleum D5762 − 18a, 2021, pp. 1–6, https://doi.org/10.1520/D5762-18A.2.

[54] R Core Team, R: A language and environment for statistical computing. R Foundation for Statistical Computing, Vienna, Austria, 2021.

[55] M.M. Clark, Transport Modeling for Environmental Engineers and Scientists, Wiley, New York City, NY, 2009.

[56] Jon Gustafsson, Visual MINTEQ ver. 3.1, 2020. https://vminteq.lwr.kth.se/.

[57] S. Iman Shayan, N. Zalivina, M. Wang, S.J. Ergas, Q. Zhang, Dynamic model of algal-bacterial shortcut nitrogen removal in photo-sequencing batch reactors, Algal Res. 64 (March) (2022), 102688, https://doi.org/10.1016/j.algal.2022.102688.

[58] E.B. Mackay, H. Feuchtmayr, M.M. De Ville, S.J. Thackeray, N. Callaghan, M. Marshall, G. Rhodes, C.A. Yates, P.J. Johnes, S.C. Maberly, Dissolved organic nutrient uptake by riverine phytoplankton varies along a gradient of nutrient enrichment, Sci. Total Environ. 722 (2020), 137837, https://doi.org/10.1016/j.scitotenv.2020.137837.

[59] H.L. Clever, R. Battino, H. Miyamoto, Y. Yampolski, C.L. Young, IUPAC-NIST solubility data series. 103. Oxygen and ozone in water, aqueous solutions, and organic liquids (supplement to solubility data series volume 7), J. Phys. Chem. Ref. Data 43 (3) (2014), https://doi.org/10.1063/1.4883876.

[60] S. Chandra, S.K. Singh, S. Das Gupta, S.K. Sahoo, in: Note Mass Specific Oxygen Uptake in the Freshwater Catfish Wallago Attu (Bloch & Schneider, 1801) 62, 2015, pp. 137–140 (3).

[61] U.S. EPA, Method 1683: Standard Oxygen Uptake Rate in Biosolids. https://www.epa.gov/sites/default/files/2015-10/documents/method_1683_draft_2001.pdf, 2001.

[62] R.F. Weiss, Carbon dioxide in water and seawater: the solubility of a non-ideal gas, Mar. Chem. 277 (7187) (1974) 203–215, https://doi.org/10.1016/S0140-6736(61)92080-3.

[63] J. Happel, H. Brenner, Low Reynold's Number Hydrodynamics, Vol. 1, Martinus Nijhoff Publishers, The Hague, Netherlands, 1983. http://link.springer.com/.

[64] B.J.F. Biggs, S. Stokseth, Hydraulic habitat suitability for periphyton in rivers, Regul. Rivers Res. Manag. 12 (2–3) (1996) 251–261, https://doi.org/10.1002/(SICI)1099-1646(199603)12:2/3<251::AID-RRR393>3.0.CO;2-X.

[65] U. Risse-Buhl, C. Anlanger, K. Kalla, T.R. Neu, C. Noss, A. Lorke, M. Weitere, The role of hydrodynamics in shaping the composition and architecture of epilithic biofilms in fluvial ecosystems, Water Res. 127 (2017) 211–222, https://doi.org/10.1016/j.watres.2017.09.054.

[66] J.P. Pacheco, C. Calvo, C. Aznarez, M. Barrios, M. Meerhoff, E. Jeppesen, A. Baattrup-Pedersen, Periphyton biomass and life-form responses to a gradient of discharge in contrasting light and nutrients scenarios in experimental lowland streams, Sci. Total Environ. 806 (2022), 150505, https://doi.org/10.1016/j.scitotenv.2021.150505.

[67] M. Graba, S. Sauvage, F.Y. Moulin, G. Urrea, S. Sabater, J.M. Sanchez-Pérez, Interaction between local hydrodynamics and algal community in epilithic biofilm, Water Res. 47 (7) (2013) 2153–2163, https://doi.org/10.1016/j.watres.2013.01.011.

[68] J.R.C. Gorospe, M.A. Juinio-Meñez, P.C. Southgate, Effects of shading on periphyton characteristics and performance of sandfish, Holothuria scabra Jaeger 1833, juveniles, Aquaculture 512 (July) (2019), https://doi.org/10.1016/j.aquaculture.2019.734307.

[69] G. Kazanjian, S. Brothers, J. Köhler, S. Hilt, Incomplete recovery of a shallow lake from a natural browning event, Freshw. Biol. 66 (6) (2021) 1089–1100, https://doi.org/10.1111/fwb.13701.

[70] M. Hondzo, H. Wang, Effects of turbulence on growth and metabolism of periphyton in a laboratory flume, Water Resources Research 38 (12) (2002), https://doi.org/10.1029/2002wr001409, pp. 13-1–13-19.

[71] J.M. Chern, S.P. Yang, Oxygen transfer rate in a coarse-bubble diffused aeration system, Ind. Eng. Chem. Res. 42 (25) (2003) 6653–6660, https://doi.org/10.1021/ie030396y.